Remote Sensing in Ecology and Conservation
Open Access
ZSL

RESEARCH ARTICLE

Precipitation and temperature drive woody vegetation dynamics in the grasslands of sub-Saharan Africa

Francesco D'Adamo[1,2], Rebecca Spake[3], James M. Bullock[4], Booker Ogutu[1], Jadunandan Dash[1] & Felix Eigenbrod[1]

[1]School of Geography and Environmental Sciences, University of Southampton, SO17 1BJ Southampton, Hampshire, UK
[2]Centre for Research on Ecology and Forestry Applications (CREAF), 08193 Cerdanyola del Vallès, Barcelona, Spain
[3]School of Biological Sciences, University of Reading, Whiteknights Campus, RG6 6AH Reading, Berkshire, UK
[4]UK Centre for Ecology & Hydrology, OX10 8BB Wallingford, Oxfordshire, UK

Keywords
grassland ecosystems, grassland-savanna-forest transition, microwave-based vegetation optical depth, remote sensing, structural equation modeling, woody dynamics

Correspondence
Francesco D'Adamo, Centre for Research on Ecology and Forestry Applications (CREAF), 08193 Cerdanyola del Vallès, Barcelona, Spain. Tel: 0034664458028. E-mail: f.dadamo@creaf.uab.cat

Funding information
This work was funded by the European Research Council Starting Grant SCALEFORES (515825101) granted to F Eigenbrod and the UKCEH National Capability project (06895) to JM Bullock.

Editor: Prof. Nathalie Pettorelli
Associate Editor: Henrike Schulte to Buhne

Received: 31 January 2025; Revised: 11 June 2025; Accepted: 16 June 2025

doi: 10.1002/rse2.70018

Remote Sensing in Ecology and Conservation 2025;**11** (6):740–754

Abstract

Identifying the drivers of ecosystem dynamics, and how responses vary spatially and temporally, is a critical challenge in the face of global change. Grasslands in sub-Saharan Africa are vital ecosystems supporting biodiversity, carbon storage, and livelihoods through grazing. However, despite their importance, the processes driving change in these systems remain poorly understood, as cross-scale interactions among drivers produce complex, context-dependent dynamics that vary across space and time. This is particularly relevant for woody vegetation dynamics, which are often linked to degradation processes (e.g., woody encroachment), with consequences for biodiversity, forage availability, and fire regimes. Here, we used satellite data and structural equation models to investigate the effects of rainfall, temperature, fire, and population density on woody vegetation dynamics in four African grassland regions (the Sahel grasslands, Greater Karoo and Kalahari drylands, Southeast African subtropical grasslands, and Madagascar) during 1997–2016. Across all regions, rainfall was consistently positively correlated with increased woody vegetation, while higher temperatures were associated with decreased woody vegetation, suggesting that water availability promotes woody plant growth, whereas rising aridity limits it. Unexpectedly, fire had a negative effect on woody cover only in the Greater Karoo and Kalahari drylands, while in Madagascar, higher temperatures and greater population density reduced fire; yet these relationships did not translate into significant indirect effects on woody vegetation. These findings illustrate the complex ways by which environmental and anthropogenic drivers shape woody vegetation dynamics in grasslands across sub-Saharan Africa. Compared to savannas, fire plays a weaker and more region-specific role in grasslands, where its feedback with woody cover is less consistent. The opposing effects of rainfall and temperature may currently constrain woody expansion, but climate change could disrupt this balance and further weaken fire's limited regulatory role. These differences highlight the need for management strategies tailored to the distinct climate–vegetation dynamics of grassland systems.

Introduction

Understanding how global environmental change will affect natural ecosystem dynamics is a central challenge in ecology. Gaining such understanding is made difficult by the complexity of natural systems, with changes that are often context-dependent across space and time (Spake et al., 2022) due to cross-scale interactions among drivers (Spake et al., 2019). Grasslands are a key biome for which context dependency in the drivers affecting ecosystem dynamics is common yet poorly understood (Bardgett et al., 2021; Li et al., 2024).

Grassy ecosystems, including grasslands and savannas, comprise approximately one-third of terrestrial ecosystems and are subject to widespread degradation that is leading to increasing concern for both biodiversity and human well-being (Bardgett et al., 2021; Strömberg & Staver, 2022). This is particularly true for the African continent, where grassy ecosystems constitute the dominant vegetation cover, host diverse endemic faunas and flora, and provide a multitude of material and non-material benefits to humans (Osborne et al., 2018). Here, dominant drivers of loss and degradation include climate change, conversion to cropland or forest, fire suppression, and overgrazing (Parr et al., 2024; Stevens et al., 2022). In addition, interactions among these drivers often trigger degradation processes. Woody plant encroachment, for instance, impoverishes grassy ecosystems as woody vegetation replacing the grass layer pushes the system toward a secondary state (e.g., shrubland, woodland) (Nerlekar & Veldman, 2020) with lower herbaceous plant diversity and palatability (Venter et al., 2017; Wieczorkowski & Lehmann, 2022).

Understanding the drivers of grassy ecosystem dynamics and their interactions over time and space is essential for improving predictions of how these ecosystems will respond to global environmental change and ultimately preventing their degradation (Abdi et al., 2022). However, this is complex due to the numerous direct and indirect processes related to climate, soil, and disturbances (Pausas & Bond, 2020), and because grassy ecosystems encompass both grasslands and savannas, that is, two distinct sub-ecosystems where these processes may not operate in the same way (Bardgett et al., 2021).

Grasslands are ecosystems dominated by indigenous (i.e., native) or natural (i.e., established through natural processes such as seed dispersal by wind or animals) grass species, differing from savannas, which are transitional woody–herbaceous systems between grassland and forest (Allen et al., 2011). Grasslands exist below 650–1000 mm of annual rainfall (mm/year), while forests generally occur above 2500 mm/year (Aleman et al., 2020; Mayer & Khalyani, 2011). Savannas are found between these ranges, with the grassland–savanna–forest transition largely determined by interactions between rainfall, vegetation, and fire (Pausas & Bond, 2020). Shady, rainy environments inhibit flammable conditions and hamper grass growth, which suppresses fire and promotes woody plant establishment (Wei, Wang, Brandt, et al., 2020). In contrast, seasonal rainfall sustains open systems promoting the colonization of flammable grasses, which in turn intensifies fires and excludes woody plants at rates that may vary with different rainfall accumulation periods before the fire season (Archibald et al., 2009). Accordingly, the feedback between fire and woody vegetation is generally negative, that is, one suppresses the other. However, the interplay between rainfall, vegetation, and fire is more complex and influenced by other drivers. Intensive rainfall before or after the core wet season, for instance, can promote woody over grassy vegetation (Brandt et al., 2019). Meanwhile, increasing temperature could trigger fires either by facilitating seasonal fuel curing or as C_4 grasses have high-temperature photosynthesis, which leads to fast biomass build-up in warmer ecosystems (Lehmann et al., 2014). Yet the opposite was also observed, as a recent sequence of drought years caused a decrease in fuel loads and fire events (Wei, Wang, Fu, et al., 2020). Further, anthropogenic factors such as land cover changes, increasing atmospheric CO_2, and management practices can also have either positive or negative effects on woody vegetation and fire activity (Alvarado et al., 2020; Hansen et al., 2013).

These examples highlight that while we know the overall drivers of woody vegetation dynamics in grassy ecosystems for sub-Saharan Africa, the degree to which their effects change across space and time remains unclear. Part of this inconsistency may relate to the fact that, generally, large-scale studies do not explicitly assess grasslands but rather consider grasslands and savannas together or investigate ecosystems based on aridity levels. This potentially conflates any different responses these two types of grassy ecosystems may have to changes in climate, disturbances, and their interactions. Remote sensing offers a powerful tool to address this challenge by providing accessible, spatially explicit, and repetitive observations of environmental and anthropogenic variables, aiding in the assessment of various ecological processes in grasslands and savannas as distinct ecosystems (Masenyama et al., 2022). While optical-based indexes such as the normalized difference vegetation index, the enhanced vegetation index, and the leaf area index are widely used resources for grassland dynamic assessments (Wang et al., 2022), recent studies have highlighted the effectiveness of other remote sensing technologies (e.g., microwave-based, hyperspectral, or very high-resolution data) in investigating terrestrial ecosystems and enhancing monitoring capabilities (e.g., Brandt et al., 2018, 2020; Brown et al., 2024). However, these technologies remain underutilized in grassland studies (Ali et al., 2016). Here we used microwave- and optical-based satellite data and structural equation models (SEMs) to quantify the relative importance of environmental and anthropogenic variables in driving woody dynamics across major grasslands of sub-Saharan Africa. Through a hypothesis-driven approach, we examined both direct and indirect (i.e., mediated by fire) effects of these variables, aiming to identify regional pathways determining the likelihood of grasslands transitioning to a woody state. We hypothesized a prevailing direct role of

rainfall on woody vegetation and fire. Similarly, we anticipated negative feedback between fire and woody vegetation and dry season rainfall to promote woody vegetation. We did not have any specific expectations regarding direct or indirect effects of temperature and human population density on woody vegetation. We did not try to anticipate to what extent support for each hypothesis varied across space and time. These hypotheses are based on the literature for grassy ecosystems in general, so they may be less relevant for grasslands. Understanding if this is the case is a key focus of our study.

Materials and Methods

Study area

The European Space Agency (ESA) Climate Change Initiative (CCI) Land Cover programme aims to maximize the potential of long-term satellite data to produce accurate land cover classification for effective land dynamic and climate modeling studies. The ESA CCI land cover map (v2.0.7, 300 m spatial resolution) describes the land surface in 22 classes following the United Nations Land Cover Classification System (UN-LCCS) (ESA, 2017). Here we used this product to define grasslands in sub-Saharan Africa by selecting classes 110 (mosaic herbaceous cover >50% and tree and shrub <50%) and 130 (grassland) and excluding areas dominated by croplands, trees, or where the herbaceous cover is lower than 50%. By doing so, we were able to produce a strict grassland mask that (i) fits our interest in naturally grass-dominated ecosystems (as opposed to more mixed grass-tree savanna regions) and (ii) matches the classification of grassland of the Intergovernmental Panel on Climate Change (ESA, 2017). Later, to account for context-dependency (e.g., ecological and climatic heterogeneity that exists across Africa, distinct socio-ecological histories among regions), we opted to subdivide grasslands by applying the One Earth Bioregions framework (One Earth, 2020). This framework aggregates similar (Dinerstein et al., 2017) terrestrial ecoregions into larger-scale ecological systems that are therefore better suited for broad regional assessments (e.g., our study). The four One Earth Bioregions are Sahel Acacia savannas (hereafter referred to as Sahel grasslands for clarity), Greater Karoo and Kalahari drylands, Southeast African subtropical grasslands, and Madagascar (Fig. 1). More preprocessing information on how we produced the grassland mask is reported in Appendix S1.

Data

Table 1 provides an overview of the key features of the datasets used in this study. All data were resampled to a common spatial resolution of 25 km × 25 km, the coarsest among our datasets, using the aggregate and resample functions from the R package 'terra' (Hijmans et al., 2022). Our analysis covers the period from 1997 to 2016, which corresponds to the time span available across all datasets.

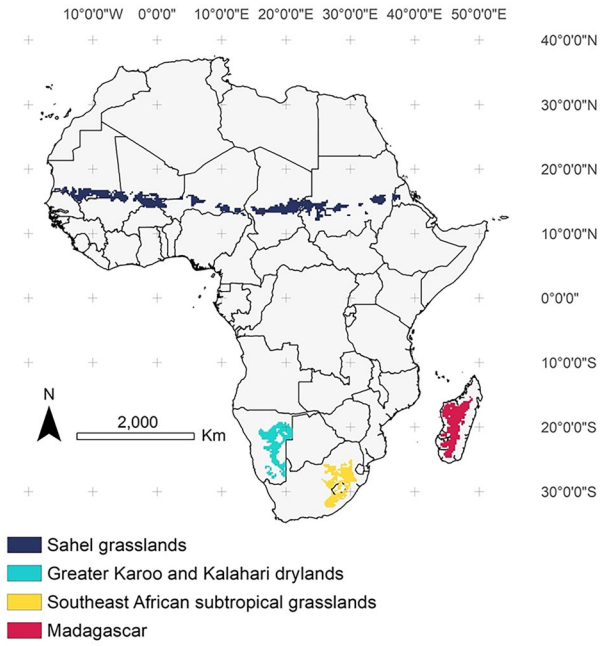

Figure 1. Grassland extent as obtained from the ESA CCI land cover map (classes 110, i.e., herbaceous cover >50% and tree and shrub <50%, and 130, i.e., grassland) and indicated by the One Earth framework (One Earth, 2020). The four bioregions are Sahel grasslands (780 pixels), Greater Karoo and Kalahari drylands (287 pixels), Southeast African subtropical grasslands (271 pixels), and Madagascar (319 pixels) (see also Appendix S1).

Vegetation optical depth (VOD) describes the attenuation of the microwave signal by the vegetation layer (Meesters et al., 2005). It is proportional to the vegetation water content of aboveground vegetation, so higher VOD values indicate high vegetation water content and more energy attenuation (e.g., dense vegetation), whereas lower VOD values refer to limited vegetation water content, little attenuation, and higher transmissivity (e.g., sparse vegetation) (Chaparro et al., 2024). Compared to optical-based products, VOD is insensitive to atmospheric haze and dust, cloud cover, or sun illumination (Li et al., 2021). We used the VOD Climate Archive (VODCA) Ku band (18.70–19.35 GHz) to exploit the longest available time series and because of its good level of agreement with other VOD, leaf area index, and vegetation continuous field global products (Moesinger et al., 2020). Here we took annual minimum values to reduce the effects of the green herbaceous layer and

Table 1. The datasets used for our analysis and their main characteristics. Rainfall data were used to calculate annual sums as well as dry season rainfall (see Appendix S2).

Name	Data	Time series	Resolution	References
VODCA	VOD (unitless)	1987–2017	Monthly 25 km × 25 km	Moesinger et al. (2020)
GFED	Burned area (ha)	1997–2016	Monthly 25 km × 25 km	van der Werf et al. (2017)
CHIRPS	Rainfall (mm $year^{-1}$)	1981 to near present	Daily 5 km × 5 km	Funk et al. (2015)
	Dry season rainfall (mm)			
CHELSA	Temperature (°C)	1980–2019	Monthly 1 km × 1 km	Karger et al. (2017)
ESA CCI SM	Soil moisture (m^3 m^{-3})	1987–2016	Daily 25 km × 25 km	Dorigo et al. (2017)
GPW	Population density (persons km^{-2})	1995–2020	Annual 1 km × 1 km	CIESIN (2018)

Abbreviations: CHELSA, Climatologies at High Resolution for the Earth's Land Surface Areas; CHIRPS, Climate Hazards Group Infrared Precipitation with Stations; ESA CCI SM, European Space Agency Climate Change Initiative for Soil Moisture; GFED, Global Fire Emissions Database; GPW, Gridded Population of the World (see text for more details); VODCA, Vegetation Optical Depth Climate Archive.

produce a VOD signal that is more representative of the general woody cover community (e.g., shrubs, small trees, large trees). This is a common approach in remote sensing-based assessments of arid and semi-arid ecosystems (e.g., Andela et al., 2013, 2017; Brandt et al., 2017; D'Adamo et al., 2021; Forkel et al., 2019), as supported by previous studies showing strong agreement between VOD and in-situ measurements of woody vegetation in drylands (Tian et al., 2016, 2017). Burned area data were obtained from the Global Fire Emissions Database (GFED), v4s. This product provides burned area from GFED4 complemented with the contribution of small fires (s), among other data (e.g., fire carbon, dry matter emissions) (van der Werf et al., 2017). Burned area represents a direct estimate of fire impacts on ecosystems and has the advantage of persisting on the land surface, thus preventing potential fire data gaps due to cloud and smoke cover spells (Andela et al., 2017). We first converted monthly burned area fraction (dimensionless) to monthly burned area (ha) using the ancillary grid map (m^2) that is embedded with the data and, second, we aggregated monthly burned area into annual sum composites. Daily rainfall data from Climate Hazards group Infrared Precipitation with Stations (CHIRPS v2.0) (Funk et al., 2015) were used to produce annual sums (mm $year^{-1}$) and to calculate the dry season rainfall (Liebmann et al., 2012) (Appendix S2). Uncertainty assessments based on mean absolute error have shown that CHIRPS data outperform many other products, including both those that incorporate gauge stations and those that do not, as well as reanalysis data (Beck et al., 2017; Funk et al., 2015). Temperature data were obtained from the Climatologies at High resolution for the Earth's Land Surface Areas (CHELSA v2.1) (Karger et al., 2017). Compared to the deprecated v1.2 version, CHELSA v2.1 replaces ERA-Interim with ERA5 reanalysis atmospheric temperature as input. This shift introduced a change in the lapse rate calculation, now based on pressure levels between 950 and 850 hPa rather than across the entire atmosphere (Karger et al., 2021). While this change may affect high-altitude regions where temperature gradients are steeper, it is unlikely to influence the results for low-altitude areas, such as the grasslands investigated here, where temperature variation with elevation is less pronounced. Validation exercises have shown that CHELSA v2.1 achieves similar accuracy to other global temperature products (Karger et al., 2017). Monthly data from daily means of synoptic hourly temperature at 2 metres were converted from Kelvin to Celsius and then averaged to produce annual mean composites. Soil moisture data were taken from the ESA CCI program (Dorigo et al., 2017). Produced as an active, passive, and active-passive merged product, we used the merged product (v04.2) as it combines the advantages of active (better for averagely vegetated areas) and passive (preferable over sparse vegetation and at distinguishing between wet and dry soils) observations (Gruber et al., 2019). We created annual soil moisture composites by summing only good quality daily data (i.e., pixels without issues) each year (m^3 m^{-3}). Soil moisture data were used to assess the role of soil moisture on woody vegetation and the effect of moisture availability on fire (Lehmann et al., 2014). The Gridded Population of the World (GPWv4) dataset provides spatially explicit global distribution of the human population (CIESIN, 2018). GPWv4 data do not rely on ancillary data sources (e.g., land cover, vegetation indices), thus precluding potential problems of collinearity with VOD (Brandt et al., 2017). We used population density data (persons km^{-2}) adjusted to the 2015 revision of the United Nations World Population Prospects to investigate the effect of people on woody vegetation and fire dynamics (Archibald et al., 2010; Brandt et al., 2017). A continuous population density time

series was produced using the available data (i.e., 2000, 2005, 2010, 2015, and 2020) to interpolate missing years (Abel et al., 2020).

Statistical analysis

Structural equation modeling (SEM) is a probabilistic tool that allows the inclusion of multiple dependent and independent variables with different distributions in a single framework (Lefcheck, 2016). Unlike standard regression, SEM is capable of evaluating both direct and indirect effects among variables, which is typical within complex natural ecosystems (Fan et al., 2016). Here we used an SEM approach as it is a useful tool for testing causal relationships hypothesized from theory and knowledge (Lehmann et al., 2014). Our statistical modeling workflow consisted of four steps:

1. *Hypotheses*: We reviewed the literature on direct and indirect relationships among variables in the grassland-savanna-forest transition (Fig. 2A) (see Introduction). Based on this, we created an initial most plausible hypothesis (represented by a causal structure), which we then modified to both simpler and more complex hypotheses to account for all ecologically reasonable combinations among variables (corresponding to alternative causal structures) (Fig. 2B). This exercise also allowed us to assess whether simpler SEMs are able to explain grassland dynamics better than more complex ones. We ended up with a total of 37 plausible hypotheses, each of which was formalized as an individual causal SEM structure (Appendix S3). All SEMs have VOD as the main response variable, with the effect of the other variables quantified directly and/or indirectly via burned area. Two exceptions were dry season rainfall and previous year VOD, which we deemed reasonable predictors of VOD only (Brandt et al., 2019) and were not included as indirect predictors of VOD to avoid any circular causality problems (Bowman et al., 2015). Annual rainfall was specified as a predictor of both VOD and burned area. We acknowledge that fire regimes may be better explained by rainfall preceding the fire season, yet we only used annual rainfall as it was strongly collinear (Pearson's $r > 0.774$) with rainfall metrics accumulated over 6, 12, 18, and 24 months before the fire season (Appendix S4) (Karp et al., 2023).
2. *Model runs*: All SEMs were run using the psem function in the R package 'piecewiseSEM' (Lefcheck et al., 2020). Rather than fitting continent-wide models with all years, separate models were fit for each bioregion (i.e., Sahel grasslands, Greater Karoo and Kalahari drylands, Southeast African subtropical grasslands, and Madagascar) and year (i.e., 1997–2016) to be able to account for both the spatial and temporal dependency structures of the data and, importantly, to assess to what extent support for each hypothesis varied across space and time. Preliminary model runs revealed strong spatial autocorrelation (SAC) in the residuals, indicated by statistically significant ($P < 0.001$) Moran's I values and correlograms (Dormann et al., 2007). To account for SAC, SEMs were embedded with spatial autoregressive error models produced with the errorsarlm function in the R package 'spatialreg' (Bivand, Piras, et al., 2022). Errorsarlm models handle SAC through spatial weighting matrices computed as the Euclidean distance between neighboring sites (i.e., pixels) (Bivand & Wong, 2018). We calculated spatial weighting matrices using the dnearneigh function from the R package 'spdep' (Bivand, Altman, et al., 2022), setting the lower and upper distance bounds at 0 and 39 km, respectively (39 km is the distance that allows all pixels to be linked to at least another pixel, including some farther pixels at the edge of the bioregions). The upper distance bound of 39 km did not vary significantly across bioregions as the data are regularly gridded (Appendix S5). SEM path coefficients were calculated as standardized regression coefficients (β) to enhance comparability across responses of different units. The indirect effect of a variable on VOD was calculated by multiplying the β coefficients of the two respective paths.
3. *Model selection*: We used Fisher's C and chi-squared (χ^2) goodness of fit measures to identify SEM specifications that best reproduce the relationships among the variables in the sample data (hereafter well-fitted SEMs). Fisher's C is calculated as negative two times the sum of the natural logarithms of the p-values from all unspecified paths, and a resulting $P > 0.05$ suggests that the model is well structured (i.e., no paths are missing) (Haynes et al., 2022). Similarly, χ^2 tests whether there is a discrepancy between the model-implied and observed covariance matrices, and also in this case $P > 0.05$ is recommended (Fan et al., 2016). In each year and each bioregion, we therefore selected only SEMs showing $P > 0.05$ for Fisher's C and χ^2. The number of well-fitted SEMs was then refined by calculating the difference in the Akaike information criterion (ΔAIC) between each SEM and the SEM with the lowest AIC (Cade, 2015) and selecting only SEMs with ΔAIC <3 (hereafter final SEMs) (Burnham et al., 2011). We present the results for each bioregion by performing natural model averaging of the final SEM β coefficients both annually with 95% confidence intervals (CIs) and averaging over the entire 1997–2016 period. We took this approach as the values of the statistically significant β coefficients did not

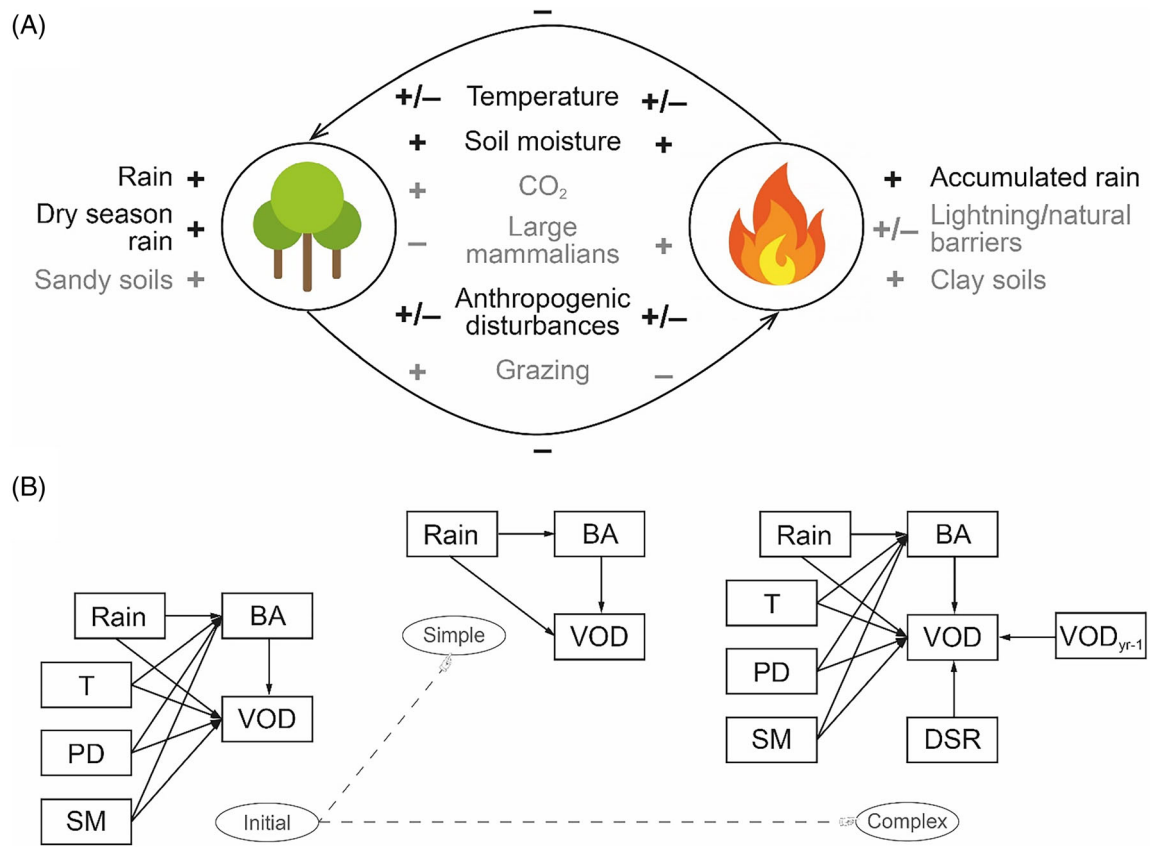

Figure 2. The key elements in the grassland-savanna-forest transition as commonly reported in the literature (see Introduction) and their described overall effect (positive (+), negative (–), or both (+/–)) on woody vegetation and fire (in gray are the variables excluded from the analysis as not available for our study regions during 1997–2016) (A). The initial hypothesis (left), and an example of a simpler (middle) and more complex (right) hypothesis as indicated by the corresponding SEM causal structure. Vegetation optical depth (VOD) is the main response variable. Burned area (BA) is both a predictor and response variable. Other variables are annual rainfall (Rain), temperature (T), dry season rainfall (DSR), population density (PD), soil moisture (SM), and previous year VOD (VOD_{yr-1}). The full list of the 37 SEM causal structures is reported in Appendix S3 (B).

change appreciably over time (coefficient of variations <5%). Effects were classified as weak, moderate, or strong depending on whether their absolute mean was below one, between one and two, or above two standard deviations, respectively. Full results for each bioregion, including the list of final SEMs, Fisher's C with P-values, chi-squared with P-values, degrees of freedom, ΔAIC, Nagelkerke R^2, β coefficients with P-values and 95% CIs, as well as the standard deviation and coefficient of variation of β coefficients for each year, are reported in Appendix S6.

4. *Model evaluation*. Although final SEMs were selected via satisfactory Fisher's C, χ^2, and ΔAIC values, we further evaluated them by calculating Nagelkerke r^2 and plotting residuals against fitted values for each variable included and not included in the model, latitude and longitude, and time (Zuur & Ieno, 2016) (Appendix S7). This step is important to assess the goodness of fit of any saturated SEMs (i.e., all variables are linked), as these have no degrees of freedom (Cortina et al., 2017). The four-step statistical modeling workflow is shown in Fig. 3.

The preprocessing we computed before the statistical analysis is detailed in Appendix S8. All analyses were performed within the R environment, version 4.2.1 (Posit Team, 2023).

Results

Only about 12% of our 37 hypothesized SEM causal structures could satisfy the criteria for selection as final SEMs each year (Tables S6.1, S6.3, S6.5, S6.7). Notably, simple SEM structures were systematically excluded from this subset, indicating that the observed direct and indirect relationships were better captured by the more complex structures.

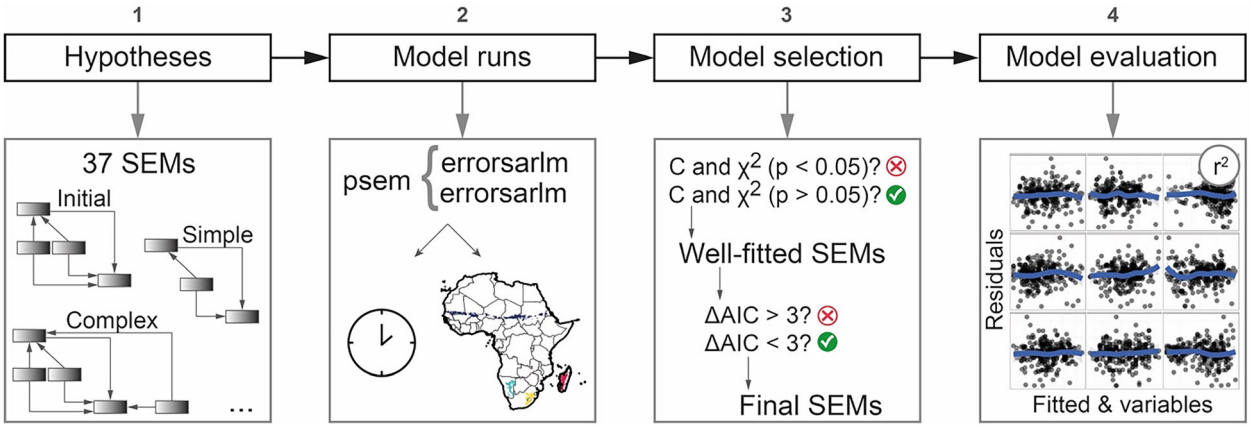

Figure 3. The four-step statistical modeling workflow. Thirty-seven hypotheses were tested by fitting spatial autoregressive error models within a structural equation modeling (SEM) framework in each year and each bioregion. Well-fitted SEMs were identified by means of satisfactory Fisher's C and χ^2 goodness of fit measures. From well-fitted SEMs, we selected final SEMs based on ΔAIC value. Final SEMs were further evaluated using Nagelkerke r^2 and residual plots.

In Sahel grasslands, rainfall showed a strong positive direct effect on both VOD (average $\beta = 0.216$) and burned area ($\beta = 0.256$) (Fig. 4A). VOD showed a moderate negative direct relationship with temperature ($\beta = -0.216$) while being largely unaffected by other variables. As expected, previous year's VOD was a strong predictor of VOD ($\beta = 0.511$) (Fig. 4A and Table S6.2). The Greater Karoo and Kalahari drylands and Southeast African subtropical grasslands showed overall similar relationships regarding the effects of rainfall on VOD and burned area, temperature on VOD, and previous year's VOD on VOD (β coefficients of the remaining relationships were largely negligible) (Fig. 4B,C and Tables S5.4 and S5.6). In addition, in the Greater Karoo and Kalahari drylands, we also found a weak negative direct effect ($\beta = -0.031$) of burned area on VOD. This is likely because the Greater Karoo and Kalahari drylands are the only bioregion where VOD significantly increased during 1997–2016, which indicates a potential increase in woody vegetation and, therefore, stronger feedback with burned area (Fig. S9.2). Madagascar also featured a positive relationship between rainfall and both VOD ($\beta = 0.126$) and burned area ($\beta = 0.208$) and a moderate negative direct effect of temperature on VOD ($\beta = -0.037$), yet here, we observed a strong negative direct effect of both temperature ($\beta = -0.429$) and population density ($\beta = -0.354$) on burned area (Fig. 4D and Table S6.8). Noticeably, both these variables showed a sharp change during 1997–2016 (Fig. S9.4).

Three key features were shared by all bioregions. First, we did not observe any significant indirect effects (i.e., mediated by burned area) of the variables on VOD. In Sahel grasslands, for instance, the indirect effect of rainfall on VOD was much weaker ($\beta = 0.256 \times 0.012 = 0.0031$) than its direct effect ($\beta = 0.216$) (Fig. 4A). This finding applied also in the case of strong direct effects of variables on burned area (e.g., temperature and population density in Madagascar) (Fig. 4D). Second, we noticed that the direct effects of precipitation and temperature on VOD had similar magnitudes but opposite signs. Given the marginal role of other variables, these diametrically opposite effects might have constrained changes in VOD, except for the Greater Karoo and Kalahari drylands. Finally, all final SEMs showed both satisfactory residual plots (Appendix S7) and explained a high degree of variation in VOD as indicated by high Nagelkerke r^2 values, that is, $r^2 = 0.88$ in Sahel grasslands, $r^2 = 0.96$ in Greater Karoo and Kalahari drylands, $r^2 = 0.84$ in Southeast African subtropical grasslands, and $r^2 = 0.94$ in Madagascar (Fig. 4A–D and Tables S6.1, S6.3, S6.5, S6.7). The high Nagelkerke r^2 values are likely related to the strong spatial autocorrelation component observed in the gridded data and, hence, to the high explanatory power of the spatial weighting distances, which statistically control for this autocorrelation, in our models.

Discussion

Ecological systems are complex because of the many interactions among biotic and abiotic components that occur at different spatiotemporal scales (Spake et al., 2019). As such, scientists tend to characterize ecological relationships as context-dependent (Spake et al., 2023) or with narrative descriptions of relationships (Zellmer et al., 2006). Our results, however, help disentangle this complexity for grassland systems by clarifying the role of temperature, rainfall, fire, and population density on woody dynamics at broad spatiotemporal scales.

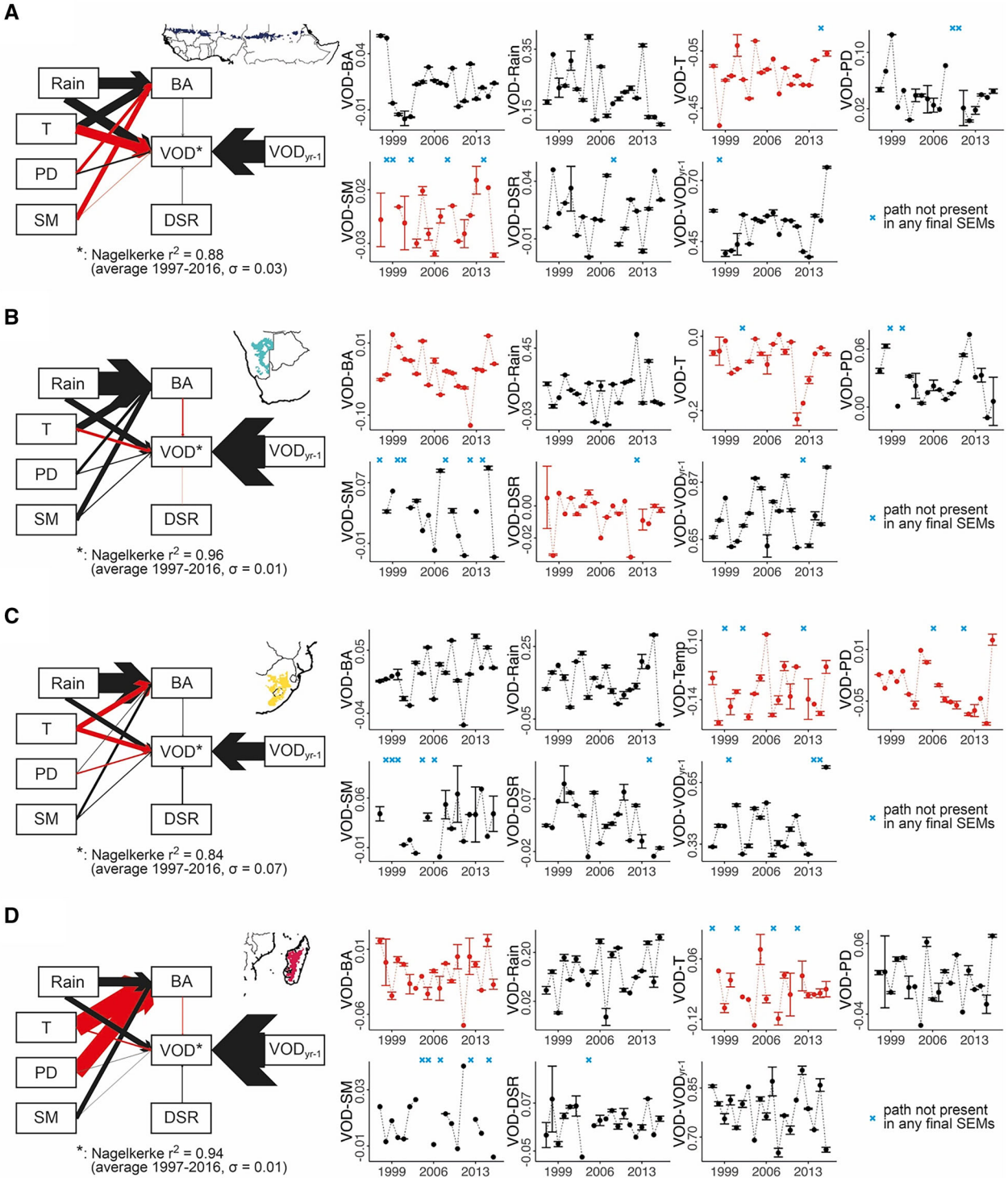

Figure 4. Final structural equation models (SEM) of the direct and indirect effects (i.e., mediated by burned area) of burned area (BA), annual rainfall (Rain), temperature (T), dry season rainfall (DSR), population density (PD), soil moisture (SM), and previous year VOD (VOD_{yr-1}) on vegetation optical depth (VOD) (left) and standardized regression coefficient (β) with 95% CIs during 1997–2016 (right) for Sahel grasslands (A), Greater Karoo and Kalahari drylands (B), Southeast African subtropical grasslands (C), and Madagascar (D). The thickness of the arrows is scaled to the β coefficients, which are calculated by natural model averaging the final SEMs in each year and later during 1997–2016. Black represents positive effect and red represents negative effect. Cyan crosses indicate years in which all available final SEM structures did not include the path between the two variables. No CIs for years with only one available β coefficient. The direct effects of rainfall and temperature on VOD are similar but opposite in sign (positive and negative, respectively) in all bioregions. Overall, no significant relationships were observed between burned area and VOD. The indirect effects of any variable on VOD were negligible. Full details are reported in Appendix S6.

In addition, they also provide empirical evidence of complexity. The low number of final SEMs each year, for instance, indicates that only specific combinations of variables yield meaningful explanations of woody dynamics. Further, final SEMs are systematically described by more complex structures, suggesting that simple models including only woody vegetation, burned area, and one or two other variables are not able to characterize the ecological relationships in time and space (Appendix S6).

Yet complexity does not mean that ecosystems have no common features. Rainfall controls both woody vegetation and burned area, which is expected as water availability is known to be the key resource for both plant growth (Ogutu et al., 2021) and fuel availability (Lehmann et al., 2014; Staver et al., 2017) in arid and semi-arid regions of Africa. However, and contradicting our initial hypothesis, dry season rainfall did not predict woody vegetation dynamics, suggesting that the establishment of woody plants in these bioregions is more related to rainfall totals (García Criado et al., 2020) than rainfall timing (Brandt et al., 2019). This is likely because the four grassland regions investigated here received very little rainfall during the dry season, implying that the wet season rain largely corresponds to annual rainfall (Appendix S4). In contrast to rainfall, temperature showed a consistent negative effect on woody vegetation. While this is unsurprising as rainy days are generally colder, climate change-driven rising aridity may cause woody plants to be more prone to hydraulic failure (Abel et al., 2023). Notably, precipitation and temperature had overall comparable but diametrically opposite effects on woody vegetation, potentially contributing to the prevention of encroachment, as indicated by the limited changes observed in VOD during 1997–2016 (Appendix S9). This result partly contradicts previous studies showing sharper increases in VOD in the drylands of the Sahel (Brandt et al., 2017; Moesinger et al., 2020). However, this discrepancy likely stems from differences in land cover data, as results can vary depending on the product or masking approach used to define the study area. Additionally, time series differences may also play a role, as trends in vegetation indices and biophysical variables depend on the period analyzed. For example, recent research has shown that different ecosystem indicators exhibited distinct trends before and after 2000, ultimately influencing overall trend calculations (Ogutu et al., 2021). Notwithstanding this, our results indicate that any future imbalance between precipitation and temperature may push the system toward a woody state, a risk that becomes increasingly relevant under ongoing climate change. Projections for Africa indicate rising temperatures and more frequent droughts, while rainfall patterns are expected to become more variable across the continent (Osborne et al., 2018), likely disrupting the balance between water availability and thermal stress and potentially tipping grassland systems toward woody-dominated landscapes. This transition appears already underway in the Greater Karoo and Kalahari drylands, that is, the only bioregion with a clear, positive VOD trend, where rising temperatures and stable precipitation may be driving woody plant proliferation (Fig. S9.2). While an increase in VOD independent of rainfall contradicts conventional understanding of woody vegetation dynamics, other studies have documented similar patterns of expansion not primarily driven by rainfall (D'Adamo et al., 2021). Contributing factors include low population growth rates (Brandt et al., 2017), rising anthropogenic CO_2 levels (Saintilan & Rogers, 2015), and shifts in both high and low herbivory pressure (Venter et al., 2018; Ward et al., 2014). Additionally, the observed decline in burned area, potentially due to fire suppression, land fragmentation, or shifts in traditional burning practices (He et al., 2019), reinforces this trend, as reduced fire activity is known to promote woody encroachment (Fig. 4B and Fig. S9.2) (Andela et al., 2017). Ultimately, the negative feedback between woody vegetation and fire appears less widespread in grasslands than savanna ecosystems of sub-Saharan Africa, emerging only at higher VOD levels, as observed in the Greater Karoo and Kalahari drylands. This evidence underscores the importance of distinguishing between these two ecosystems, as the weaker fire-woody vegetation feedback of grasslands may reduce the capacity of fire to regulate woody cover, a

limitation that could become more pronounced under global environmental change. Previous studies have reached similar conclusions, reporting a sharp increase in tree density across a broad rainfall gradient, even where fire regimes have remained historically stable (Case & Staver, 2017). This suggests that controlling woody encroachment may require fire frequencies exceeding historical levels. However, such an approach conflicts with livestock grazing, which reduces fire intensity by depleting fuel loads, potentially forcing land managers to choose between maintaining grazing productivity and preventing ecosystem transition to a woody state (Case & Staver, 2017). Madagascar also displayed a few distinct features, that is, the effect of temperature and human population density on fire (Fig. S9.4). This may relate not only to the different geographical setting (i.e., island vs. continental) but also to widespread human activities in the country (Ralimanana et al., 2022). Unsustainable agriculture and overexploitation, for instance, are likely explanations for our results, as fragmented landscapes reduce fuel connectivity and, therefore, fire spread (Bowman et al., 2020). Further, these anthropogenic activities (e.g., clearing woody vegetation) may explain why fire decline did not trigger woody encroachment (Phelps et al., 2022).

Conclusions

Broad, remote sensing-based ecological studies are invaluable for complementing local-scale research and generalizing patterns, processes, and interactions into broader predictions. In this study, we were specifically interested in naturally grass-dominated ecosystems, rather than savannas, to analyze their woody dynamics, a task that required a careful approach to biome classification. While variations in classification approaches and methods make it challenging to unequivocally distinguish biomes using remote sensing-based land cover products, our procedure, based on pure grassland classes from the ESA CCI land cover map (Fig. 1 and Appendix S1), provided new insights into the role of environmental and anthropogenic factors in shaping long-term woody dynamics in the major grasslands of sub-Saharan Africa. Unsurprisingly, precipitation was a key driver of woody vegetation dynamics and fire, whereas the relationship between fire and woody cover that is well-documented in savannas appeared to be less significant in grasslands, suggesting that grassland fire management practices may need distinct approaches from those used in savannas. The weak relationship with fire is perhaps surprising given our inclusion of pixels with up to 49% woody vegetation. However, if anything, this inclusion would bias our results toward stronger fire-woody vegetation feedback, thereby strengthening confidence in our findings. Despite the weaker relationship between fire and woody cover in grasslands, we did not observe significant woody encroachment in our study area (except for Greater Karoo and Kalahari drylands), indicating that other factors may be equally important in maintaining a grassland state. Therefore, while fire management remains important, it should be implemented as part of an approach that accounts for these interacting drivers (McLauchlan et al., 2020). Temperature consistently exhibited a negative effect on woody vegetation, while dry season rainfall, population density, and soil moisture had only minor influences. Overall, the role of these drivers in controlling woody vegetation dynamics was consistent across space and time, yet changes or interactions for one or more variables in Greater Karoo and Kalahari drylands and Madagascar led to local, context-dependent patterns that need to be accounted for to plan effective grassland management (Bullock et al., 2021; Lu et al., 2024). On the other hand, it is also possible that some patterns might have resulted from variables not investigated here (e.g., atmospheric CO_2, grazing, soil texture, etc.) (Case & Staver, 2018; Stevens et al., 2017). Another caveat to our findings is that the coarse spatial resolution of VOD data did not allow us to capture finer-grain processes and changes. For instance, a surprisingly large number of non-forest trees was observed in African drylands using 10–0.5 m spatial resolution satellite data (Reiner et al., 2023). Similarly, the contribution of small fires undetectable from coarse spatial resolution products is decisive for appropriate burned area and fire emission estimations in Africa (Ramo et al., 2021). Consequently, the low resolution of our data may have constrained the detection of indirect effects in our SEMs, as higher-resolution data could reveal more significant interactions among environmental variables. Furthermore, utilizing higher spatial resolution would eliminate the need to resample land cover maps, enabling more precise biome delineation. These points suggest that the consistent availability of high-resolution remote sensing data will be essential to better understand finer-grain dynamics and, ultimately, terrestrial ecosystem distribution (Zhang et al., 2019).

Acknowledgements

We thank the groups that produced and shared the datasets used here. We thank J. Lefcheck for his resources and guidance with the CRAN package 'piecewiseSEM', R Bivand for his help with the CRAN package 'spdep', and P Fibich for the fruitful discussions on errorsarlm models. This work was funded by the European Research Council Starting Grant SCALEFORES (515825101) granted to F

Eigenbrod and the UKCEH National Capability project (06895) to JM Bullock.

Author Contributions

Francesco D'Adamo: Conceptualization; methodology; formal analysis; data curation; visualization; writing – review and editing; writing – original draft; investigation. **Rebecca Spake:** Conceptualization; writing – review and editing; methodology; data curation; supervision; investigation. **James M. Bullock:** Conceptualization; funding acquisition; writing – review and editing; methodology; supervision; investigation. **Booker Ogutu:** Writing – review and editing; methodology; conceptualization. **Jadunandan Dash:** Methodology; writing – review and editing; conceptualization. **Felix Eigenbrod:** Conceptualization; funding acquisition; writing – review and editing; methodology; project administration; supervision; formal analysis; investigation.

Conflict of Interest

The authors have no conflicts of interest to declare.

Data Availability Statement

All data supporting the findings of this study are publicly available. The preprocessed data for reproducing our analysis are available from the corresponding author upon request.

References

Abdi, A.M., Brandt, M., Abel, C. & Fensholt, R. (2022) Review article satellite remote sensing of savannas: current status and emerging opportunities. *Journal of Remote Sensing*, **2022**, 9835284. https://doi.org/10.34133/2022/9835284

Abel, C., Abdi, A.M., Tagesson, T., Horion, S. & Fensholt, R. (2023) Contrasting ecosystem vegetation response in global drylands under drying and wetting conditions. *Global Change Biology*, **29**, 3954–3969. https://doi.org/10.1111/gcb.16745

Abel, C., Horion, S., Tagesson, T., De Keersmaecker, W., Seddon, A.W.R., Abdi, A.M. et al. (2020) The human–environment nexus and vegetation–rainfall sensitivity in tropical drylands. *Nature Sustainability*, **4**, 25–32. https://doi.org/10.1038/s41893-020-00597-z

Aleman, J.C., Fayolle, A., Favier, C., Staver, A.C., Dexter, K.G., Ryan, C.M. et al. (2020) Floristic evidence for alternative biome states in tropical Africa. *Proceedings of the National Academy of Sciences of the United States of America*, **117**(45), 28183–28190. https://doi.org/10.1073/pnas.2011515117

Ali, I., Cawkwell, F., Dwyer, E., Barrett, B. & Green, S. (2016) Satellite remote sensing of grasslands: from observation to management. *Journal of Plant Ecology*, **9**(6), 649–671. https://doi.org/10.1093/jpe/rtw005

Allen, V.G., Batello, C., Berretta, E.J., Hodgson, J., Kothmann, M., Li, X. et al. (2011) An international terminology for grazing lands and grazing animals. *Grass and Forage Science*, **66**(1), 2–28. https://doi.org/10.1111/j.1365-2494.2010.00780.x

Alvarado, S.T., Andela, N., Silva, T.S.F. & Archibald, S. (2020) Thresholds of fire response to moisture and fuel load differ between tropical savannas and grasslands across continents. *Global Ecology and Biogeography*, **29**(2), 331–344. https://doi.org/10.1111/geb.13034

Andela, N., Liu, Y.Y., Van Dijk, M. & A. I. J., De Jeu, R. A. M., & McVicar, T. R. (2013) Global changes in dryland vegetation dynamics (1988-2008) assessed by satellite remote sensing: comparing a new passive microwave vegetation density record with reflective greenness data. *Biogeosciences*, **10**(10), 6657–6676. https://doi.org/10.5194/bg-10-6657-2013

Andela, N., Morton, D.C., Giglio, L., Chen, Y., Van Der Werf, G.R., Kasibhatla, P.S. et al. (2017) A human-driven decline in global burned area. *Science*, **356**(6345), 1356–1362. https://doi.org/10.1126/science.aal4108

Archibald, S., Nickless, A., Govender, N., Scholes, R.J. & Lehsten, V. (2010) Climate and the inter-annual variability of fire in southern Africa: a meta-analysis using long-term field data and satellite-derived burnt area data. *Global Ecology and Biogeography*, **19**(6), 794–809. https://doi.org/10.1111/j.1466-8238.2010.00568.x

Archibald, S., Roy, D.P., van Wilgen, B.W. & Scholes, R.J. (2009) What limits fire? An examination of drivers of burnt area in southern Africa. *Global Change Biology*, **15**(3), 613–630. https://doi.org/10.1111/j.1365-2486.2008.01754.x

Bardgett, R.D., Bullock, J.M., Lavorel, S., Manning, P., Schaffner, U., Ostle, N. et al. (2021) Combatting global grassland degradation. *Nature Reviews Earth and Environment*, **2**(10), 720–735. https://doi.org/10.1038/s43017-021-00207-2

Beck, H.E., Vergopolan, N., Pan, M., Levizzani, V., Van Dijk, A.I.J.M., Weedon, G.P. et al. (2017) Global-scale evaluation of 22 precipitation datasets using gauge observations and hydrological modeling. *Hydrology and Earth System Sciences*, **21**(12), 6201–6217. https://doi.org/10.5194/hess-21-6201-2017

Bivand, R., Altman, M., Anselin, L., Assunção, R., Berke, O., Blanchet, G. et al. (2022) Package 'spdep'. CRAN

Bivand, R., Piras, G., Anselin, L., Bernat, A., Blankmeyer, E., Chun, Y. et al. (2022) Package 'spatialreg'. CRAN.

Bivand, R.S. & Wong, D.W.S. (2018) Comparing implementations of global and local indicators of spatial association. *TEST*, **27**(3), 716–748. https://doi.org/10.1007/s11749-018-0599-x

Bowman, D.M.J.S., Kolden, C.A., Abatzoglou, J.T., Johnston, F.H., van der Werf, G.R. & Flannigan, M. (2020) Vegetation fires in the Anthropocene. *Nature Reviews Earth and*

Environment, **1**(10), 500–515. https://doi.org/10.1038/s43017-020-0085-3

Bowman, D.M.J.S., Perry, G.L.W. & Marston, J.B. (2015) Feedbacks and landscape-level vegetation dynamics. *Trends in Ecology & Evolution*, **30**(5), 255–260. https://doi.org/10.1016/j.tree.2015.03.005

Brandt, M., Hiernaux, P., Rasmussen, K., Tucker, C.J., Wigneron, J.-P., Diouf, A.A. et al. (2019) Changes in rainfall distribution promote woody foliage production in the Sahel. *Communications Biology*, **2**(1), 133. https://doi.org/10.1038/s42003-019-0383-9

Brandt, M., Rasmussen, K., Peñuelas, J., Tian, F., Schurgers, G., Verger, A. et al. (2017) Human population growth offsets climate-driven increase in woody vegetation in sub-Saharan Africa. *Nature Ecology & Evolution*, **1**(4), 81. https://doi.org/10.1038/s41559-017-0081

Brandt, M., Tucker, C.J., Kariryaa, A., Rasmussen, K., Abel, C., Small, J. et al. (2020) An unexpectedly large count of trees in the west African Sahara and Sahel. *Nature*, **587** (August 2019), 78–82. https://doi.org/10.1038/s41586-020-2824-5

Brandt, M., Wigneron, J.P., Chave, J., Tagesson, T., Penuelas, J., Ciais, P. et al. (2018) Satellite passive microwaves reveal recent climate-induced carbon losses in African drylands. *Nature Ecology & Evolution*, **2**, 827–835. https://doi.org/10.1038/s41559-018-0530-6 Satellite.

Brown, L.A., Morris, H., MacLachlan, A., D'Adamo, F., Adams, J., Lopez-Baeza, E. et al. (2024) Hyperspectral leaf area index and chlorophyll retrieval over Forest and row-structured vineyard canopies. *Remote Sensing*, **16**(12), 2066. https://doi.org/10.3390/rs16122066

Bullock, J.M., Fuentes-Montemayor, E., McCarthy, B., Park, K., Hails, R.S., Woodcock, B.A. et al. (2021) Future restoration should enhance ecological complexity and emergent properties at multiple scales. *Ecography*, **2022**, 1–11. https://doi.org/10.1111/ecog.05780

Burnham, K.P., Anderson, D.R. & Huyvaert, K.P. (2011) AIC model selection and multimodel inference in behavioral ecology: some background, observations, and comparisons. *Behavioral Ecology and Sociobiology*, **65**, 23–35. https://doi.org/10.1007/s00265-010-1029-6

Cade, B.S. (2015) Model averaging and muddled multimodel inferences. *Ecology*, **96**(9), 2370–2382. https://doi.org/10.1890/14-1639.1

Case, M.F. & Staver, A.C. (2017) Fire prevents woody encroachment only at higher-than-historical frequencies in a South African savanna. *Journal of Applied Ecology*, **54**(3), 955–962. https://doi.org/10.1111/1365-2664.12805

Case, M.F. & Staver, A.C. (2018) Soil texture mediates tree responses to rainfall intensity in African savannas. *New Phytologist*, **219**(4), 1363–1372. https://doi.org/10.1111/nph.15254

Chaparro, D., Jagdhuber, T., Piles, M., Jonard, F., Fluhrer, A., Vall-llossera, M. et al. (2024) Vegetation moisture estimation in the Western United States using radiometer-radar-lidar synergy. *Remote Sensing of Environment*, **303**, 113993. https://doi.org/10.1016/j.rse.2024.113993

CIESIN (2018) Documentation for the Gridded Population of the World, Version 4 (GPWv4), Revision 11 Data Sets. In *Columbia University* (53 pp). NASA Socioeconomic Data and Applications Center (SEDAC). https://doi.org/10.7927/H45Q4T5F.

Cortina, J.M., Green, J.P., Keeler, K.R. & Vandenberg, R.J. (2017) Degrees of freedom in SEM: are we testing the models that we claim to test? *Organizational Research Methods*, **20**(3), 350–378. https://doi.org/10.1177/1094428116676345

D'Adamo, F., Ogutu, B., Brandt, M., Schurgers, G. & Dash, J. (2021) Climatic and non-climatic vegetation cover changes in the rangelands of Africa. *Global and Planetary Change*, **202**, 103516. https://doi.org/10.1016/j.gloplacha.2021.103516

Dinerstein, E., Olson, D., Joshi, A., Vynne, C., Burgess, N.D., Wikramanayake, E. et al. (2017) An ecoregion-based approach to protecting half the terrestrial realm. *Bioscience*, **67**(6), 534–545. https://doi.org/10.1093/biosci/bix014

Dorigo, W., Wagner, W., Albergel, C., Albrecht, F., Balsamo, G., Brocca, L. et al. (2017) ESA CCI soil moisture for improved earth system understanding: state-of-the art and future directions. *Remote Sensing of Environment*, **203**, 185–215. https://doi.org/10.1016/j.rse.2017.07.001

Dormann, F.C., McPherson, M.J., Araújo, B.M., Bivand, R., Bolliger, J., Carl, G. et al. (2007) Methods to account for spatial autocorrelation in the analysis of species distributional data: a review. *Ecography*, **30**(5), 609–628. https://doi.org/10.1111/j.2007.0906-7590.05171.x

ESA (2017) Land Cover CCI: product user guide. Version 2.0, 105.

Fan, Y., Chen, J., Shirkey, G., John, R., Wu, S.R., Park, H. et al. (2016) Applications of structural equation modeling (SEM) in ecological studies: an updated review. *Ecological Processes*, **5**(1), 19. https://doi.org/10.1186/s13717-016-0063-3

Forkel, M., Dorigo, W., Lasslop, G., Chuvieco, E., Hantson, S., Heil, A. et al. (2019) Recent global and regional trends in burned area and their compensating environmental controls. *Environmental Research Communications*, **1**(5), 051005. https://doi.org/10.1088/2515-7620/ab25d2

Funk, C., Peterson, P., Landsfeld, M., Pedreros, D., Verdin, J., Shukla, S. et al. (2015) The climate hazards infrared precipitation with stations—a new environmental record for monitoring extremes. *Scientific Data*, **2**, 150066. https://doi.org/10.1038/sdata.2015.66

García Criado, M., Myers-Smith, I.H., Bjorkman, A.D., Lehmann, C.E.R. & Stevens, N. (2020) Woody plant encroachment intensifies under climate change across tundra and savanna biomes. *Global Ecology and Biogeography*, **29**(5), 925–943. https://doi.org/10.1111/geb.13072

Gruber, A., Scanlon, T., van der Schalie, R., Wagner, W. & Dorigo, W. (2019) Evolution of the ESA CCI soil moisture climate data records and their underlying merging methodology. *Earth System Science Data*, **11**(2), 717–739. https://doi.org/10.5194/essd-11-717-2019

Hansen, M.C., Potapov, P.V., Moore, R., Hancher, M., Turubanova, S.A., Tyukavina, A. et al. (2013) High-resolution global maps of 21st-century Forest cover change. *Science*, **342**(6160), 850–853. https://doi.org/10.1126/science.1244693

Haynes, K.J., Liebhold, A.M., Lefcheck, J.S., Morin, R.S. & Wang, G. (2022) Climate affects the outbreaks of a forest defoliator indirectly through its tree hosts. *Oecologia*, **198**, 407–418. https://doi.org/10.1007/s00442-022-05123-w

He, T., Lamont, B.B. & Pausas, J.G. (2019) Fire as a key driver of Earth's biodiversity. *Biological Reviews*, **94**(6), 1983–2010. https://doi.org/10.1111/brv.12544

Hijmans, R. J., Bivand, R., Forner, K., Pebesma, E. & Sumner, M. D. (2022) Package "terra." In CRAN.

Karger, D.N. Conrad, O. Böhner, J. Kawohl, T. Kreft, H. Soria-Auza, R.W. et al. (2021) Climatologies at high resolution for the Earth land surface areas In CHELSA V2.1: Technical specification.

Karger, D.N., Conrad, O., Böhner, J., Kawohl, T., Kreft, H., Soria-Auza, R.W. et al. (2017) Climatologies at high resolution for the earth's land surface areas. *Scientific Data*, **4**, 1–20. https://doi.org/10.1038/sdata.2017.122

Karp, A.T., Uno, K.T., Berke, M.A., Russell, J.M., Scholz, C.A., Marlon, J.R. et al. (2023) Nonlinear rainfall effects on savanna fire activity across the African humid period. *Quaternary Science Reviews*, **304**, 107994. https://doi.org/10.1016/j.quascirev.2023.107994

Lefcheck, J., Byrnes, J. & James, G. (2020) Package "piecewiseSEM". CRAN.

Lefcheck, J.S. (2016) piecewiseSEM: piecewise structural equation modelling in r for ecology, evolution, and systematics. *Methods in Ecology and Evolution*, **7**(5), 573–579. https://doi.org/10.1111/2041-210X.12512

Lehmann, C.E.R., Anderson, T.M., Sankaran, M., Higgins, S.I., Archibald, S., Hoffmann, W.A. et al. (2014) Savanna vegetation-fire-climate relationships differ among continents. *Science*, **343**(6170), 548–552. https://doi.org/10.1126/science.1247355

Li, X., Wigneron, J.P., Frappart, F., Fan, L., Ciais, P., Fensholt, R. et al. (2021) Global-scale assessment and inter-comparison of recently developed/reprocessed microwave satellite vegetation optical depth products. *Remote Sensing of Environment*, **253**(December 2020), 112208. https://doi.org/10.1016/j.rse.2020.112208

Li, X., Zuo, X., Qiao, J., Hu, Y., Wang, S., Yue, P. et al. (2024) Context-dependent impact of changes in precipitation on the stability of grassland biomass. *Functional Ecology*, **38**, 1185–1198. https://doi.org/10.1111/1365-2435.14539

Liebmann, B., Bladé, I., Kiladis, G.N., Carvalho, L.M.V., Senay, G.B., Allured, D. et al. (2012) Seasonality of African precipitation from 1996 to 2009. *Journal of Climate*, **25**(12), 4304–4322. https://doi.org/10.1175/JCLI-D-11-00157.1

Lu, T., Zhang, W., Abel, C., Horion, S., Brandt, M., Huang, K. et al. (2024) Changes in vegetation-water response in the Sahel-Sudan during recent decades. *Journal of Hydrology: Regional Studies*, **52**, 101672. https://doi.org/10.1016/j.ejrh.2024.101672

Masenyama, A., Mutanga, O., Dube, T., Bangira, T., Sibanda, M. & Mabhaudhi, T. (2022) A systematic review on the use of remote sensing technologies in quantifying grasslands ecosystem services. *GIScience & Remote Sensing*, **59**(1), 1000–1025. https://doi.org/10.1080/15481603.2022.2088652

Mayer, A.L. & Khalyani, A.H. (2011) Grass trumps trees with fire. *Science*, **334**(6053), 188–189. https://doi.org/10.1126/science.1213908

McLauchlan, K.K., Higuera, P.E., Miesel, J., Rogers, B.M., Schweitzer, J., Shuman, J.K. et al. (2020) Fire as a fundamental ecological process: research advances and frontiers. *Journal of Ecology*, **108**(5), 2047–2069. https://doi.org/10.1111/1365-2745.13403

Meesters, A.G.C.A., DeJeu, R.A.M. & Owe, M. (2005) Analytical derivation of the vegetation optical depth from the microwave polarization difference index. *IEEE Geoscience and Remote Sensing Letters*, **2**(2), 121–123. https://doi.org/10.1109/LGRS.2005.843983

Moesinger, L., Dorigo, W., De Jeu, R., Van Der Schalie, R., Scanlon, T., Teubner, I. et al. (2020) The global long-term microwave Vegetation Optical Depth Climate Archive (VODCA). *Earth System Science Data*, **12**(1), 177–196. https://doi.org/10.5194/essd-12-177-2020

Nerlekar, A.N. & Veldman, J.W. (2020) High plant diversity and slow assembly of old-growth grasslands. *Proceedings of the National Academy of Sciences of the United States of America*, **117**(31), 18550–18556. https://doi.org/10.1073/pnas.1922266117

Ogutu, B.O., D'Adamo, F. & Dash, J. (2021) Impact of vegetation greening on carbon and water cycle in the African Sahel-Sudano-Guinean region. *Global and Planetary Change*, **202**, 103524. https://doi.org/10.1016/j.gloplacha.2021.103524

One Earth (2020) Bioregions https://www.oneearth.org/

Osborne, C.P., Charles-Dominique, T., Stevens, N., Bond, W.J., Midgley, G. & Lehmann, C.E.R. (2018) Human impacts in African savannas are mediated by plant functional traits. *New Phytologist*, **220**, 10–24. https://doi.org/10.1111/nph.15236

Parr, C.L., Te Beest, M. & Stevens, N. (2024) Conflation of reforestation with restoration is widespread. *Science*, **383**(6684), 698–701. https://doi.org/10.1126/science.adj0899

Pausas, J.G. & Bond, W.J. (2020) Alternative biome states in terrestrial ecosystems. *Trends in Plant Science*, **25**(3), 250–263. https://doi.org/10.1016/j.tplants.2019.11.003

Phelps, L.N., Andela, N., Gravey, M., Davis, D.S., Kull, C.A., Douglass, K. et al. (2022) Madagascar's fire regimes challenge global assumptions about landscape degradation. *Global Change Biology*, **28**, 1–6960. https://doi.org/10.1111/gcb.16206

Posit Team. (2023) *RStudio: Integrated Development Environment for R*. Boston, MA: Posit Software, PBC. http://www.posit.co/

Ralimanana, H., Perrigo, A.L., Smith, R.J., Borrell, J.S., Faurby, S., Rajaonah, M.T. et al. (2022) Madagascar's extraordinary biodiversity: threats and opportunities. *Science*, **378**(6623), eadf1466. https://doi.org/10.1126/science.adf1466

Ramo, R., Roteta, E., Bistinas, I., van Wees, D., Bastarrika, A., Chuvieco, E. et al. (2021) African burned area and fire carbon emissions are strongly impacted by small fires undetected by coarse resolution satellite data. *Proceedings of the National Academy of Sciences of the United States of America*, **118**(9), 1–7. https://doi.org/10.1073/pnas.2011160118

Reiner, F., Brandt, M., Tong, X., Skole, D., Kariryaa, A., Ciais, P. et al. (2023) More than one quarter of Africa's tree cover is found outside areas previously classified as forest. *Nature Communications*, **14**(1), 2258. https://doi.org/10.1038/s41467-023-37880-4

Saintilan, N. & Rogers, K. (2015) Woody plant encroachment of grasslands: a comparison of terrestrial and wetland settings. *New Phytologist*, **205**(3), 1062–1070. https://doi.org/10.1111/nph.13147

Spake, R., Bellamy, C., Graham, L.J., Watts, K., Wilson, T., Norton, L.R. et al. (2019) An analytical framework for spatially targeted management of natural capital: supplementary. *Nature Sustainability*, **2**(2), 90–97. https://doi.org/10.1038/s41893-019-0223-4

Spake, R., Bowler, D.E., Callaghan, C.T., Blowes, S.A., Doncaster, C.P., Antão, L.H. et al. (2023) Understanding 'it depends' in ecology: a guide to hypothesising, visualising and interpreting statistical interactions. *Biological Reviews*, **98**, brv.12939. https://doi.org/10.1111/brv.12939

Spake, R., O'Dea, R.E., Nakagawa, S., Doncaster, C.P., Ryo, M., Callaghan, C.T. et al. (2022) Improving quantitative synthesis to achieve generality in ecology. *Nature Ecology & Evolution*, **6**(12), 1818–1828. https://doi.org/10.1038/s41559-022-01891-z

Staver, A.C., Botha, J. & Hedin, L. (2017) Soils and fire jointly determine vegetation structure in an African savanna. *New Phytologist*, **216**(4), 1151–1160. https://doi.org/10.1111/nph.14738

Stevens, N., Bond, W., Feurdean, A. & Lehmann, C.E.R. (2022) Grassy ecosystems in the Anthropocene. *Annual Review of Environment and Resources*, **47**, 16.1–16.29.

Stevens, N., Lehmann, C.E.R., Murphy, B.P. & Durigan, G. (2017) Savanna woody encroachment is widespread across three continents. *Global Change Biology*, **23**(1), 235–244. https://doi.org/10.1111/gcb.13409

Strömberg, C.A.E. & Staver, A.C. (2022) The history and challenge of grassy biomes. *Science*, **377**(6606), 592–593. https://doi.org/10.1126/science.add1347

Tian, F., Brandt, M., Liu, Y.Y., Rasmussen, K. & Fensholt, R. (2017) Mapping gains and losses in woody vegetation across global tropical drylands. *Global Change Biology*, **23**(4), 1748–1760. https://doi.org/10.1111/gcb.13464

Tian, F., Brandt, M., Liu, Y.Y., Verger, A., Tagesson, T., Diouf, A.A. et al. (2016) Remote sensing of vegetation dynamics in drylands: evaluating vegetation optical depth (VOD) using AVHRR NDVI and in situ green biomass data over west African Sahel. *Remote Sensing of Environment*, **177**, 265–276. https://doi.org/10.1016/j.rse.2016.02.056

van der Werf, G.R., Randerson, J.T., Giglio, L., Van Leeuwen, T.T., Chen, Y., Rogers, B.M. et al. (2017) Global fire emissions estimates during 1997-2016. *Earth System Science Data*, **9**(2), 697–720. https://doi.org/10.5194/essd-9-697-2017

Venter, Z.S., Cramer, M.D. & Hawkins, H.J. (2018) Drivers of woody plant encroachment over Africa. *Nature Communications*, **9**(1), 1–7. https://doi.org/10.1038/s41467-018-04616-8

Venter, Z.S., Hawkins, H.J. & Cramer, M.D. (2017) Implications of historical interactions between herbivory and fire for rangeland management in African savannas. *Ecosphere*, **8**, 1–14. https://doi.org/10.1002/ecs2.1946

Wang, Z., Ma, Y., Zhang, Y. & Shang, J. (2022) Review of remote sensing applications in grassland monitoring. *Remote Sensing*, **14**(12), 2903. https://doi.org/10.3390/rs14122903

Ward, D., Hoffman, M.T. & Collocott, S.J. (2014) A century of woody plant encroachment in the dry Kimberley savanna of South Africa. *African Journal of Range and Forage Science*, **31**(2), 107–121. https://doi.org/10.2989/10220119.2014.914974

Wei, F., Wang, S., Brandt, M., Fu, B., Meadows, M.E., Wang, L. et al. (2020) Responses and feedbacks of African dryland ecosystems to environmental changes. *Current Opinion in Environmental Sustainability*, **48**, 29–35. https://doi.org/10.1016/j.cosust.2020.09.004

Wei, F., Wang, S., Fu, B., Brandt, M., Pan, N., Wang, C. et al. (2020) Nonlinear dynamics of fires in Africa over recent decades controlled by precipitation. *Global Change Biology*, **26**(8), 4495–4505. https://doi.org/10.1111/gcb.15190

Wieczorkowski, J.D. & Lehmann, C.E.R. (2022) Encroachment diminishes herbaceous plant diversity in grassy ecosystems worldwide. *Global Change Biology*, **28**(18), 5532–5546. https://doi.org/10.1111/gcb.16300

Zellmer, A.J., Allen, T.F.H. & Kesseboehmer, K. (2006) The nature of ecological complexity: a protocol for building the narrative. *Ecological Complexity*, **3**(3), 171–182. https://doi.org/10.1016/j.ecocom.2006.06.002

Zhang, W., Brandt, M., Wang, Q., Prishchepov, A.V., Tucker, C.J., Li, Y. et al. (2019) From woody cover to woody canopies: how Sentinel-1 and Sentinel-2 data advance the

mapping of woody plants in savannas. *Remote Sensing of Environment*, **234**, 111465. https://doi.org/10.1016/j.rse.2019.111465

Zuur, A.F. & Ieno, E.N. (2016) A protocol for conducting and presenting results of regression-type analyses. *Methods in Ecology and Evolution*, **7**(6), 636–645. https://doi.org/10.1111/2041-210X.12577

Supporting Information

Additional supporting information may be found online in the Supporting Information section at the end of the article.

Data S1.